Recruitment, inheritance and role of downy mildew-associated microbiome in *Arabidopsis thaliana*

Written by: Hannah Ploemacher
Daily supervisor: Jelle Spooren
Examiners: Roeland Berendsen & Corné Pieterse
Utrecht University, Plant Microbe Interactions
21-9-2023

Abstract

Plants live in close association with microbes, which can help combat disease in case of infection. When infected with the obligate biotrophic oomycete *Hyaloperonospora arabidopsidis* (*Hpa*), *Arabidopsis thaliana* recruits beneficial *Hpa*-associated microbes (HAM) from naïve soil to the rhizosphere and phyllosphere, where they enhance disease resistance. This effect can be transferred to populations subsequently growing on the same soil, known as soil-borne legacy (SBL). During SBL, the HAM is inherited to the rhizosphere and phyllosphere of subsequent plant populations. This study investigates the disease-induced recruitment and soil-borne inheritance of the HAM, as it remains unclear how the HAM moves from root to shoot and what drives this recruitment.

In this study, the microbial origin of SBL was validated with an SBL assay using sterilized soil. We showed that sterilized soil does not allow SBL to take place, and amendment with natural soil recovers the ability to create SBL. Moreover, the recruitment of HAM is studied by inoculating *A. thaliana* plants with gnotobiotic *Hpa* (gno*Hpa*) and repeatedly passing phyllosphere wash-offs to new populations. Using qPCR, we quantified *Hpa* infection in these cultures. Unexpectedly, the gno*Hpa* and *Hpa* lines did not differ in *Hpa* quantity, where we expected the HAM present with *Hpa* to decrease infection. Using 16S rRNA sequencing, the phyllosphere samples are analyzed to test for the disease-induced build-up of HAM ASVs in the phyllosphere. The 16S rRNA sequencing data, which may reveal the unexpected lack of difference in the cultures, is currently still being processed.

Additionally, to test the effect of root exudates on HAM composition and recruitment, we studied root exudate mutants who have been shown to lack the ability to create SBL. We used 16S rRNA sequencing of the phyllo- and rhizosphere of an SBL assay to study the effect of root exudates on HAM composition, and visualized the recruitment of a bioluminescent *Xanthomonas*, representative to the most prominent HAM ASV *Xanthomonas* a0e1a, in a plate setup. In the SBL assay, camalexin-deficient *pad3* showed enhanced susceptibility to *Hpa* strain Noco2. However, in the bioluminescence recruitment experiment, no differential recruitment was found at 1dpi regardless of gno*Hpa* infection, or genotype. The anticipated 16S rRNA sequencing data may show a differential HAM composition as a result of camalexin deficiency.

Our results contribute to the understanding of the relationship between plants, beneficial microbes, and pathogenic oomycetes. This knowledge of disease-induced microbial recruitment will allow us to harness these organisms as biological control agents against pathogenic oomycetes in food crops, to ultimately develop more sustainable agricultural practices.

Introduction

Plants are closely surrounded by micro-organisms, both above and belowground. This plant microbiome is referred to as the plant's second genome and influences the growth and health of the plant (Turner *et al*., 2013; Berendsen *et al*., 2012). The soil area immediately surrounding plant roots, commonly referred to as the rhizosphere, is inhabited by a diverse and abundant microbial community. The carbon-rich photosynthates exuded by the plant roots facilitate a community of commensal, pathogenic and beneficial microbes that compete for these nutrients (Raaijmakers *et al*., 2009). Contrary to the rhizosphere, the aboveground plant biomass, or phyllosphere, is considered a much less favorable environment for microbes, due to nutrient limitations and strong fluctuations in temperature, light intensity and humidity (Vorholt, 2012). As a result, the phyllosphere generally accommodates lower numbers and a different palette of microbes compared to the rhizosphere (Trivedi, 2020). Finally, a limited subset of microbes that colonize niches in close proximity of plant tissues can colonize the plant interior, called the endosphere (Hardoim *et al*., 2008). The root- and leaf endosphere is separated from the plant exterior by structural and chemical barriers. The plant can therefore strictly regulate intercompartmental movement of microbes, which results in different microbial compositions and abundances in the plant in- and exterior.

Most soil-borne pathogens have to achieve sufficient numbers on their host for successful infection, and their success is therefore directly influenced by competition with surrounding microbes (Raaijmakers *et al*., 2009). Apart from this direct competition with their pathogenic counterparts, beneficial microbes may contribute to plant growth and health by priming the plant's immune responses via induced systemic resistance (ISR) (Meena *et al*., 2017; Pieterse *et al*., 2014). Recognition of microbe-associated molecular patterns (MAMPs) of root-associated beneficial microbes induces a hormonal response that puts the plant in a heightened state of defense (Boller & Felix, 2009). This process of priming costs relatively little resources but allows the plant to respond more quickly and strongly to pathogens.

To a certain extent, plants exert control on microbial community composition as the microbiome is dependent on carbon-rich compounds provided by the plant. When challenged by (a)biotic stresses, plants can adjust the blend of metabolites that are produced and exuded, thereby actively shaping the microbial communities with whom they are associated (Pascale *et al*., 2020). Metabolites of the phenylpropanoid pathway, such as coumarins, flavonoids, and camalexins, have been shown to play important roles in the recruitment and assembly of plant-associated microbial communities (Stringlis *et al*., 2019; Hassan & Mathesius, 2012; Koprivova *et al*., 2019). This is the basis of the "cry-for-help" hypothesis, which states that plants employ stress-induced recruitment of beneficial microbes as a strategy to actively select disease-suppressing soil microbiomes (Rolfe *et al*., 2019).

A prime example of disease-induced recruitment of beneficial microbes has been shown using *Arabidopsis thaliana* inoculated with the downy mildew pathogen *Hyaloperonospora arabidopsidis* (hereafter: *Hpa*) (Berendsen *et al*., 2018; Vismans *et al*., 2021; Goossens & Spooren *et al*., 2023). *Hpa* is a member of the oomycetes, which encompass many plant pathogens of economically important crops, including *Phytophtera infestans* (potato), *Hyaloperonospora brassicae* (brassica) and *Bremia lactucae* (lettuce) (Coates & Beynon, 2010). As an obligate biotrophic pathogen, *Hpa* is cultured in laboratories by weekly passaging spores from diseased plants to healthy plants. As a result, an *Hpa*-associated microbiome (HAM) is co-cultured, accompanying *Hpa* spores during inoculation (Goossens & Spooren *et al*., 2023). This HAM has evolved independently in multiple laboratories across Europe, and individual HAM-members have been shown to be isogenic. A consortium of HAM-members has been shown to promote growth and induce resistance against *Hpa* when mixed through a natural soil (Berendsen *et al*., 2018). In addition, germ-free gnotobiotic *Hpa* (gno*Hpa*) spores yield higher sporulation than regular *Hpa* spores and co-inoculating the HAM with gno*Hpa* decreases infection, indicating that the HAM reduces *Hpa* proliferation (Goossens & Spooren *et al*., 2023). Finally, when

inoculating successive plant populations with gno*Hpa*, the HAM accumulates in the rhizosphere and phyllosphere. This implies that upon *Hpa* infection, the plant specifically recruits the HAM, which is then inherited by plant populations subsequently growing on the same soil, to combat *Hpa* infection there.

Interestingly, increased resistance provided by microbes recruited upon *Hpa* infection can extend to successive plant populations. In a previous SBL assay, the response plant population showed a reduction of *Hpa* spore production when these plants were grown on soil conditioned by *Hpa*-inoculated plants, compared to soil conditioned by healthy plants (Berendsen *et al*., 2018). Thus, the accumulation of beneficial bacteria in the soil can also benefit disease resistance of subsequent plant populations growing on that same soil. This concept, dubbed soil-borne legacy of disease (SBL) (Bakker *et al*., 2018), is similar to a well described concept called disease-suppressive soils, which can occur when multiple monocultured crop generations are grown on the same soil (Raaijmakers & Mazzola, 2016). Goossens & Spooren *et al* (2023) demonstrated that both the rhizosphere and phyllosphere of plants grown on soils conditioned by *Hpa*-inoculated plants are dominated by HAM. This implies inheritance of HAM from one plant population to the next, and the transfer of HAM from soil to aboveground parts of the plant. Plant root exudates are suspected to play a role, as mutants deficient in coumarin (*myb72* and *f6'h1*), flavonoid (*tt4*) and camalexin (*pad3*) are unable to create *Hpa*-induced SBL (Vismans *et al*., 2022; Spooren & Qi *et al*., unpublished data). How these plant root exudates help modulate the root microbiome and thereby aid in the recruitment and inheritance of disease-suppressing bacteria is unknown.

In this study, we aim to gain more insight into the recruitment and inheritance of the HAM in the rhizo- and phyllosphere of *A. thaliana*. First of all, we aim to verify that SBL is indeed the result of disease-induced beneficial microbe recruitment by performing an SBL bioassay in natural soil, sterilized soil, and sterilized soil amended with natural soil. Additionally, we set out to further demonstrate that HAM buildup in *Hpa* laboratory cultures is the result of repeatedly recruiting and passaging. To this end, a mimic laboratory culture was started using gno*Hpa*, which was then passaged five times, scoring disease severity, and performing 16S rRNA sequencing to follow changes in the phyllosphere microbiome. Furthermore, an SBL assay was performed with coumarin, flavonoid, and camalexin deficient mutants, with 16S rRNA sequencing of the phyllo- and rhizosphere, to elucidate the impact of root exudates on HAM inheritance. Lastly, to gain more insight into HAM recruitment, we used a bioluminescent *Xanthomonas* strain representative to the most prominent HAM ASV *Xanthomonas* a0e1a, to visualize recruitment from rhizosphere to phyllosphere upon gno*Hpa* infection in a plate setup. Together, these experiments shed light on the *Hpa*-induced recruitment of plant-beneficial microbes, expanding the knowledge on pathogenic oomycetes, and exploring possible methods of biological control.

Material and methods

Reijerscamp soil preparation

The soil used for the soil experiments was sourced from the Reijerscamp nature reserve in the Netherlands (52°01'02.55'', 5°77'99.83''), as described by Berendsen *et al* (2018). The soil was prepared for experimental use by air drying and subsequently sieving out large debris (1-mm sieve). The dry soil was stored at room temperature before use. For the sterile soil experiment, Reijerscamp soil was sterilized by Gamma-irradiation and stored at room temperature in sealed bags.

***Arabidopsis thaliana* seed propagation**

In a watertight container, sterilized river sand was saturated with half-strength Hoagland nutrient solution (Pieterse *et al*., 1996). *A. thaliana* seeds of Col-0, Col-0 *RPP5*, *f6'h1*, *tt4*, and *pad3* were sown

on the sand by sprinkling seeds over the surface. These were incubated in a short day climate chamber (21°C, 70% relative humidity, 10 h light/14 h dark, light intensity 100 µmol m^{-2} s^{-1}).

After 14 days, 392-mL pots were filled with twice autoclaved 5:12 sand soil mix, and saturated with half-strength Hoagland nutrient solution. Three seedlings of each genotype were transplanted into each pot. These plants were placed in a long day climate chamber (21°C, 70% relative humidity, 12 h light/12 h dark, light intensity 100 µmol m^{-2} s^{-1}), where they were given half-strength Hoagland nutrient solution twice a week until the flower stalks began to dry.

Once the plants had completely dried, the seeds were harvested by repeatedly sieving the flower stalks until only the seeds remained. These were then stored in paper seed bags at room temperature.

Sowing on Reijerscamp soil

A. thaliana seeds were suspended in sterile 0.2% water agar and stratified at 4°C for 2-4 days.

60-mL pots were filled with 120 $\pm$ 2.5 g of Reijerscamp soil amended with tap water in a 1/10 ratio (v/w) until the soil was firm but not waterlogged. Pots were covered with circular green plastic cut-outs of micro pipette tip holder (Greiner Bio-One, 0.5–10 µL, Item No.: 771280) to prevent growth of algae and ensure uniform distance between seeds. The pots were placed in 12mm diameter petri dishes, transferred into trays covered with a clear lid, and stored in a cold chamber (4°C) overnight.

The next day, the pots were sown using a 1-mL pipette. The seed suspension was carefully pipetted into the holes of the covers so that 1-3 seeds were sown into each hole.

Plant growth conditions

After sowing, trays were transferred to a short day growth chamber (21°C, 70% relative humidity, 10 h light/14 h dark, light intensity 100 µmol m^{-2} s^{-1}) to germinate the seeds. Pots were watered 3mL tap water from the bottom every few days to keep the soil moist. On day 7 after germination, the plants were watered from the bottom using 5mL of half-strength Hoagland nutrient solution, and the closed lids were replaced by mesh lids to allow air flow, decreasing ambient humidity.

(gno)*Hpa* inoculation

On day 14 post sowing, the plants were inoculated with *Hpa* strain Noco2 or with a mock treatment of sterile tap water. Sporulating leaf material of *Hpa*-infected plants was collected in sterile tap water, hand shaken and filtered with Miracloth to remove residual plant material. Spore concentrations were adjusted to 50 spores μL^{-1}, unless otherwise specified in the experimental section below. Using an airbrush, the inoculum was sprayed onto the plants, until visible droplets formed on the leaves, after which the plants were left to dry for 1h. Once dry, the plants were placed in trays. To create favorable conditions for (gno)*Hpa* infection, solid, opaque lids were sprinkled with water and taped onto the trays, decreasing light intensity and ensuring high humidity. The plants were put back in the short day climate chamber (21°C, 70% relative humidity, 10 h light/14 h dark, light intensity 100 µmol m^{-2} s^{-1}) for 7 days.

Harvest and resowing

Seven days post inoculation (dpi), when clear *Hpa* sporulation could be observed, the leaf material was harvested for spore counting. Leaf material was removed using a razor and collected in tubes with 3-6 mL tap water depending on disease severity. These tubes were then hand shaken for 15 seconds to release the spores from the leaves. Disease severity was quantified by average spore counts in three 1-µL droplets using a light microscope. After the harvest of the conditioning population, the experimental cycle was repeated by sowing the stratified seeds of the response population directly on the same soil.

Gamma-irradiated soil experiment
Prior to potting and sowing, *A. thaliana* seeds were surface sterilized using chlorine gas for 3.5h. After sterilization, the seeds were stratified as described above.

Pots were prepared as described above, filled with either natural Reijerscamp soil, Gamma-irradiated Reijerscamp soil, or a mix with a ratio of 1:9 of natural to Gamma-irradiated Reijerscamp soil. Pots were prepared in the order from Gamma-irradiated, to mix, to natural, to prevent cross-contamination with soil microbes. The experimental setup is otherwise identical to that described above, so the pots were not kept sterile throughout the experiment, to ensure any significant effect is associated with soil microbes.

Plants were inoculated 14 days post sowing using either mock-solution (sterile tap water) or gno*Hpa* (50 spores μL^{-1}). Harvest was done as described above, followed by the sowing of the response population. Then, 14 days post sowing, the response population was inoculated solely with gno*Hpa* (60 spores μL^{-1}) and harvested 7 days later, determining disease severity as described above.

Passaging experiment
For the passaging experiment, pots were prepared as written above, except for the green covers, which were not used. Seeds were sown using a multichannel pipette to ensure equal distance between the seeds. New pots were made and sown every week for five consecutive weeks. The plants were grown in the short day growth chamber and received Hoagland nutrient solution after 7 days.

After 14 days, the first population of plants was inoculated with mock-solution, gno*Hpa* (80 spores μL^{-1}), or *Hpa* (80 spores μL^{-1}), or left untreated. Replicate lines were kept separate in Eco2Boxes throughout the experiment. At 7 dpi, disease severity was assessed by assigning a score from 1-5 based on the extent of visual sporulation. This scoring system was used to eliminate gno*Hpa* or *Hpa* lines that showed no sporulation, as well as mock and untreated lines that did show sporulation. Moreover, for each replicate pot and treatment, half of the phyllosphere material was sampled from equally distributed places in the pot was harvested for DNA extraction, followed by qPCR and 16S rRNA amplicon sequencing. The harvested phyllosphere material was directly flash frozen in liquid nitrogen and then stored at -80°C. The remainder of the mock, *Hpa* and *gnoHpa* phyllosphere material was passaged onto next plant populations. To this end, a leaf wash-off was prepared by harvesting the remaining leaf material of a replicate in a 2mL Eppendorf tube containing 1.6mL sterile tap water and vortexing for 15 seconds. The leaf wash-off was transferred to 2-mL spraying units and sprayed onto a pot containing the next plant population, which was then placed in a clean Eco2Box. Additionally, from the new batch of plants, a number of pots equal to the number of replicates in the inoculated lines was set aside in Eco2Boxes as the untreated control. This experimental cycle was repeated for a total of 5 passages. The experiment was stopped after passage 5, as mild sporulation occurred in 3 of the mock lines.

DNA extraction, qPCR and 16S rRNA amplicon sequencing
The phyllosphere material was tissuelyzed for DNA extraction until the material was a fine powder. DNA extraction was done using the KingFisher™ MagAttract® PowerSoil® DNA KF Kit, according to the protocol. The presence of DNA was confirmed using a Nanodrop Spectrophotometer.

To quantify disease severity, a qPCR was performed using the BioRad OPUS384 qPCR machine and *Arabidopsis* and *Hpa* actin primers: 5' AATCACAGCACTTGCACCA 3' (AtActFwd), 5' GAGGGAAGCAAGAATGGAAC 3' (AtActRv), 5' GTGTCGCACACTGTACCCATTTAT 3' (HpaActFwd), 5' ATCTTCATCATGTAGTCGGTCAAGT 3' (HpaActRv).

DNA samples were sent to Novogene CO for 16S rRNA amplicon sequencing.

HAM transmittance by soil-borne legacy deficient mutants
A. thaliana Col-0, Col-0 RPP5, *tt4*, *pad3* and *f6'h1* seeds were stratified for 4 days, and sown on natural Reijerscamp soil, prepared as described above.

The conditioning population was spray-inoculated with either mock solution (sterile tap water) or *Hpa* (65 spores μL^{-1}). Harvesting was done similarly as written above, where disease severity was quantified by spore counts, and phyllosphere samples were harveseted and stored at -80°C prior to DNA extraction.

The response population, consisting of Col-0 seeds, was sown on the pots. After 14 days, the response population was spray-inoculated with mock solution (sterile tap water). At 7 dpi, both the leaf and root material was harvested for DNA extraction. Once the leaf material was harvested, the soil was washed from the roots using tap water. The harvested leaf and root material was directly flash frozen in liquid nitrogen and then stored at -80°C.

***Xanthomonas* visualization plate preparation**
A. thaliana Col-0 seeds were sterilized for 3.5h with chloric gas and then sowed on plates with Murashige and Skoog (MS) medium with 0.5% added sucrose, pH 5.8 (Murashige & Skoog, 1962). The plates were stratified at 4°C for 2 to 4 days after which they were transferred to a short day climate chamber (21°C, 70% relative humidity, 10 h light/14 h dark, light intensity 100 µmol m^{-2} s^{-1}) for 10 days.

After 10 days, two seedlings with equal root lengths were transferred to a new MS plate with 0.5% sucrose, pH 5.8. One seedling was inoculated with gnotobiotic *Hpa* (gno*Hpa*) by dabbing its leaves with a sporulating leaf. The other seedling was not inoculated, functioning as a mock. The plates were put in a short day growth chamber (21°C, 70% relative humidity, 10 h light/14 h dark, light intensity 100 µmol m^{-2} s^{-1}) for 3 days.

When the seedlings were 13 days old, 3 dpi with gno*Hpa*, they were inoculated with bioluminescent *Xanthomonas UU (XUU)* from a 5-day-old *XUU* culture. A single colony was suspended in 10 mM $MgSO_4$ and diluted to an optical density measured at 600 nm (OD600) of 0.05. A 2-µL droplet of inoculum was placed on the root tip of each seedling. One plate was inoculated with just $MgSO_4$ as a negative control. The plates were put in the short day growth chamber and imaged every day for 5 days.

***XUU* visualization with CCD camera**
The plates were taken out of the growth room 30 min before visualization to acclimate to the darkness. Every plate was imaged with an exposure time of 60 s with 75 EM gain. A light photo was made subsequently, in order to accurately localize the bioluminescence in the plants. After imaging, the seedlings were put back in the short day growth chamber. Imaging was repeated every 24h for 5 days.

Image processing
The images of the *XUU* visualization were processed in imageJ. Brightness and contrast ratio was increased equally for all pictures. Using the Measure function, the length of the bioluminescence between inoculation droplet and root-shoot junction was determined, after scale was set to a 2-cm ruler present in a light photo.

Data analysis
Data was analyzed in RStudio, using R version 3.6.3.

Results

SBL is created by a disease-induced beneficial microbiome recruitment from natural soil

To verify that SBL is indeed the result of disease-induced beneficial microbe recruitment, and not a direct effect of plant exudates, we performed an SBL bioassay where plants were grown in natural Reijerscamp soil, Gamma-irradiated (sterile) Reijerscamp soil, and a mix with a ratio of 1:9 of natural to sterile Reijerscamp soil. The conditioning population was inoculated with either mock solution or gno*Hpa*. The response population was inoculated entirely with gno*Hpa*, and disease severity was quantified to determine which soil types facilitated SBL. Both the conditioning and response populations had similar shoot fresh weights, and disease severity in the conditioning populations was equal in all soil types (Fig S1).

Response plants grown on natural gno*Hpa*-conditioned soils developed significantly lower gno*Hpa* spore counts ($P < 0.05$, one-tailed Welch's *t*-test) than plants grown on natural mock-conditioned soils (Fig. 1), supporting previous findings on the disease suppressive effect of SBL. In sterile soil, this disease suppressive phenotype is lost ($P > 0.05$, one-tailed Welch's *t*-test), whereas supplementing sterile soil with 10% natural soil remediates the increased resistance ($P < 0.05$, one-tailed Welch's *t*-test). These results indicate that the presence of soil microbes is required to create SBL and excludes a direct effect of plant-exuded chemicals.

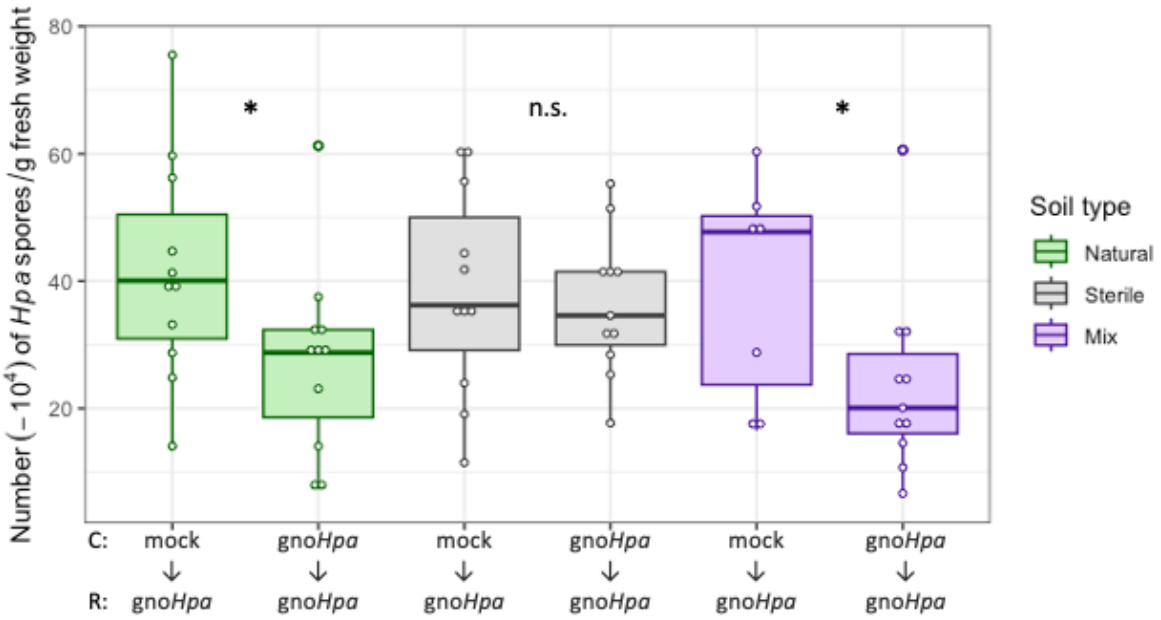

Figure 1. Disease severity in number (-10^4) of *Hpa* spores corrected for shoot fresh weight, of the gno*Hpa*-inoculated response population grown in natural, sterile, or mix soil. The x-axis shows the conditioning (C) and response (R) treatments. Within each soil type, statistically significant decreases of *Hpa* spore counts compared to mock spore counts are indicated with an asterisk, as determined with a one-tailed Welch's *t*-test ($P < 0.05$).

Repeated passaging of gno*Hpa* and *Hpa* increases disease severity over time

To demonstrate that HAM buildup in *Hpa* laboratory cultures is the result of repeated HAM recruitment when passaging *Hpa*, this laboratory culture was simulated by starting with gno*Hpa*, *Hpa* and mock inoculums, passaging the phyllosphere microbiome and (gno)*Hpa* spores every week, and harvesting phyllosphere samples weekly for qPCR and 16S rRNA sequencing.

Figure 2 shows the ratio of (gno)*Hpa* and *A. thaliana* DNA per week for the gno*Hpa* and *Hpa* lines as a measure of disease. In week 2, the gno*Hpa* line had a significantly higher infection than the *Hpa* line ($P < 0.05$, one-tailed Welch's *t*-test) (Fig. 2A). Although not significant, week 1 shows a similar trend of

higher infection in the gno*Hpa* line compared to the *Hpa* line (P = 0.13, one-tailed Welch's *t*-test). These results are in line with expectations, based on previous research (Goossens & Spooren *et al*., 2023). However, in the other weeks, the gno*Hpa* line was not significantly more infected than the *Hpa* line (P > 0.05, one-tailed Welch's *t*-test), as gno*Hpa* and *Hpa* quantities equalized in week 3, 4 and 5. Over the course of the experiment, both the gno*Hpa* and *Hpa* line show an increase in (gno)*Hpa* infection (Fig. 2B). In the gno*Hpa* line, week 5 plants had a significantly higher *Hpa*/*At* DNA ratio compared to week 1 plants (P < 0.05, Tukey's post-hoc test). Similarly, week 4 and 5 plants in the *Hpa* line had significantly higher *Hpa/At* DNA ratios compared to week 1 plants (P < 0.05, Tukey's post-hoc test).

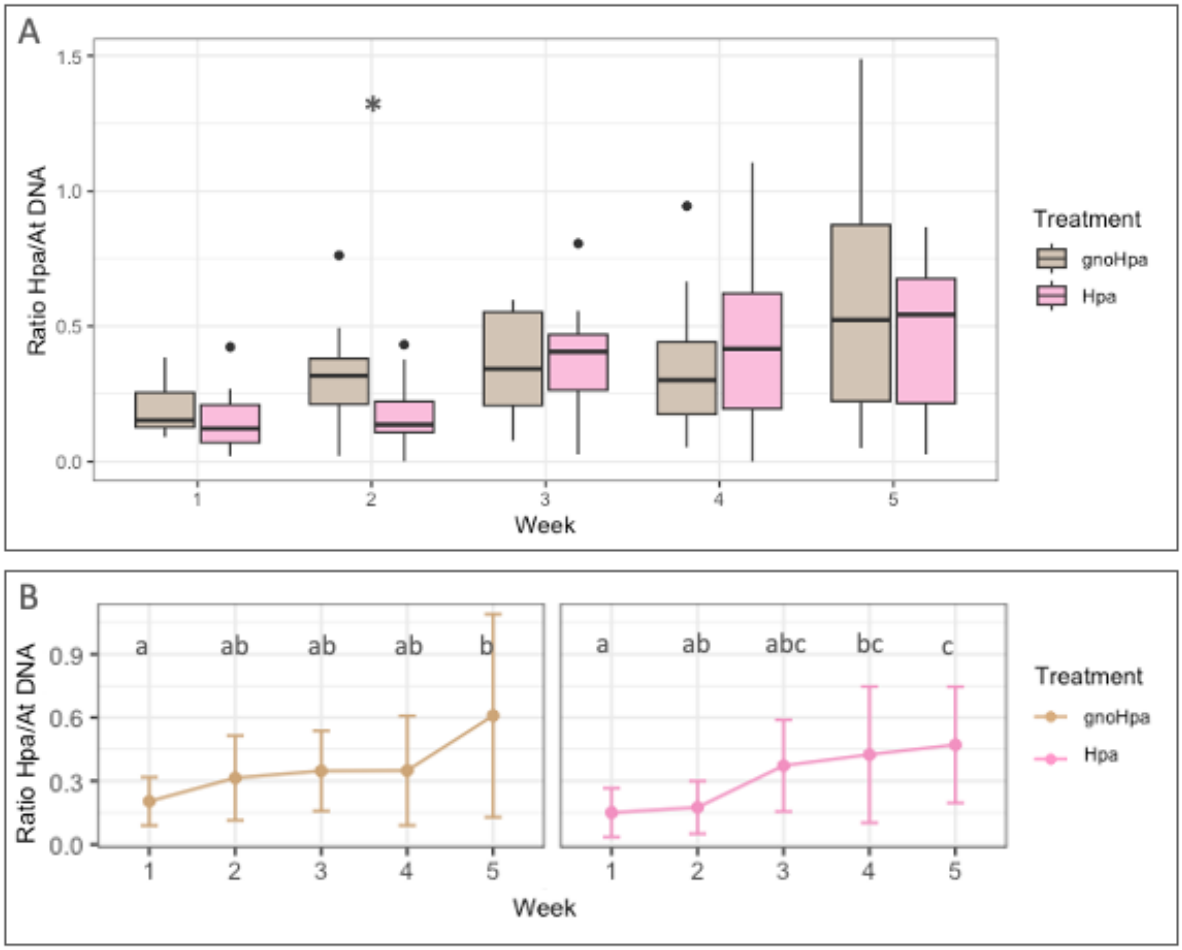

Figure 2. A) Weekly (gno)*Hpa* infection rate, quantified by the ratio of *Hpa/At* DNA, of gno*Hpa* and *Hpa* inoculated plants. In week 2, the ratio of *Hpa*/*At* DNA was significantly higher in gno*Hpa* inoculated plants than in *Hpa* inoculated plants (P < 0.05, one-tailed Welch's *t*-test). In week 1 and 3-5, gno*Hpa* inoculated plants were not significantly more infected than *Hpa* inoculated plants (P > 0.05, one-tailed Welch's *t*-test). B) Weekly gno(*Hpa*) infection of gno*Hpa* and *Hpa* lines, quantified by the ratio of *Hpa/At* DNA. Significant differences are indicated by different letters (P < 0.05, Tukey's post-hoc test).

The gradual increase in (gno)*Hpa* infection rate is likely the result of the natural proliferation of *Hpa*, through the production of sporangia carrying many spores. Indeed, in almost every week, the *Hpa*/At ratio correlates significantly with the *Hpa*/At ratio of the week before (Fig. S2). This indicates that generally, a significant part of (gno)*Hpa* infection rate in any week can be explained by the infection rate of the previous week. To correct for this cumulative effect, we adjusted the *Hpa*/At ratio of each week for the *Hpa*/At ratio of the previous week, defining this as the *Hpa* infection success rate. Figure 3 shows the *Hpa* infection success rate for individual replicates in the gno*Hpa* (G) and *Hpa* (H) lines over the course of five passages. The dashed line indicates the infection success rate at the start of the experiment, which equals 1. An infection success rate higher than 1 indicates an increase in (gno)*Hpa* infection severity, whereas lower than 1 indicates a decrease in (gno)*Hpa* infection severity.

The unadjusted individual replicates show varying patterns of overall increase in *Hpa*/At ratio (Fig. S3). However, when adjusted for the infection rate in the previous week, the (gno)*Hpa* infection success rate does not appear to be a linear increase over the course of the experiment. Most replicates have peaks where the (gno)*Hpa* infection success rate is 2 to 4 times higher than at the start of the experiment. Interestingly, the gno*Hpa* replicates appear to experience more fluctuations over the course of the experiment compared to the *Hpa* replicates, perhaps indicating more variability, or less stability in the phyllosphere microbiome. The anticipated 16S rRNA sequencing data will reveal whether these fluctuations in (gno)*Hpa* infection success rate are indeed correlated with changes in the phyllosphere microbiome. Of particular interest are replicates that have a (gno)*Hpa* infection success rate lower than 1, as their phyllosphere microbial composition may reveal a disease suppressive microbiome.

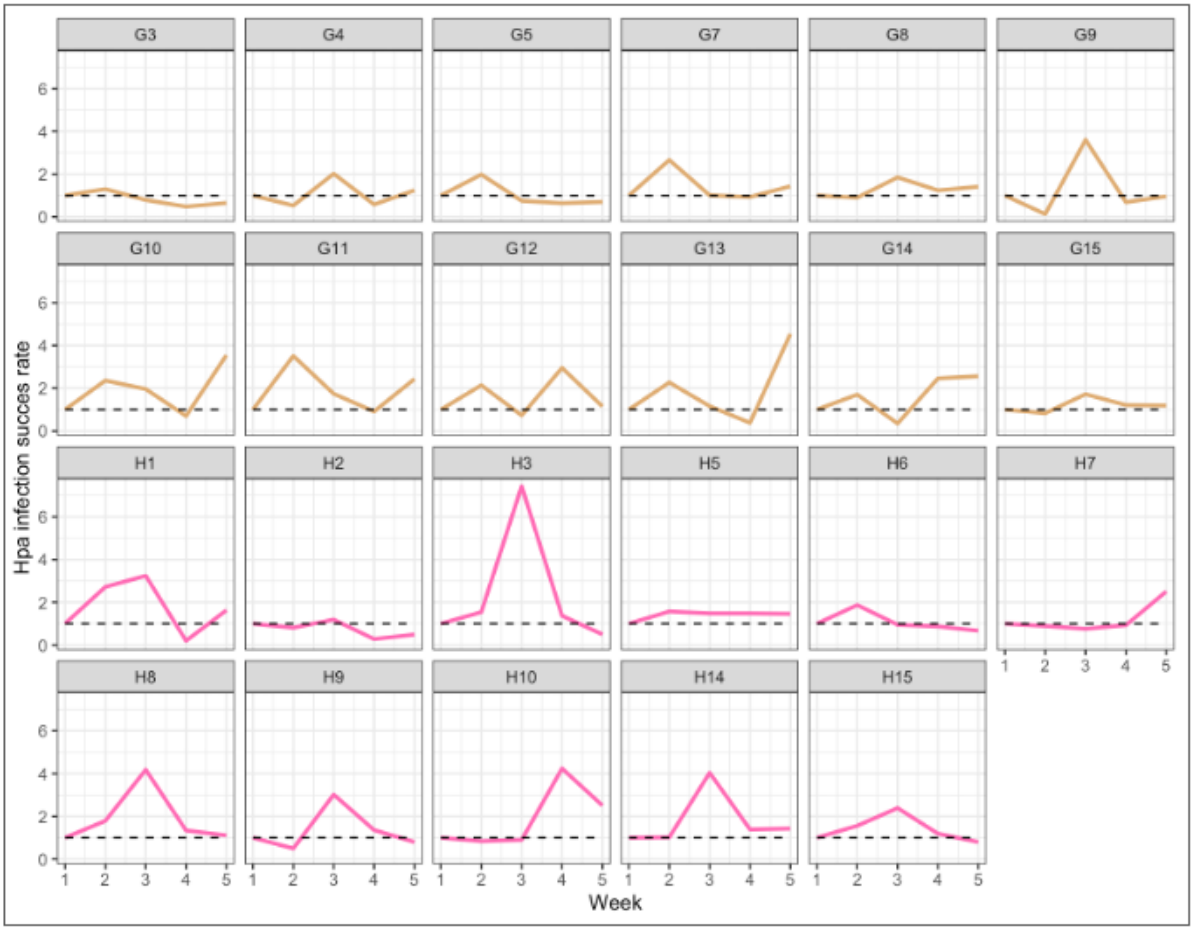

Figure 3. Weekly *Hpa* infection success rate, which is the *Hpa*/At ratio adjusted for the *Hpa*/At ratio of the previous week, in individual replicates of gno*Hpa* (G, orange) and *Hpa* (H, pink) lines. The dashed line indicates the initial *Hpa* infection success rate, which equals 1.

Camalexin deficient mutant *pad3* is hypersusceptible to *Hpa* strain Noco2

The coumarin, flavonoid and camalexin deficient mutants *f6'h1*, *tt4* and *pad3*, respectively, have previously been shown to lack the ability to create SBL. To study the influence of these root exudates on the disease-induced recruitment of beneficial microbes that is necessary for SBL, *A. thaliana* genotypes Col-0, Col-0 RPP5, *f6'h1*, *tt4* and *pad3* were grown on natural Reijerscamp soil and inoculated with *Hpa* or mock solution. The DNA samples of the conditioning population phyllosphere, and the response population phyllo- and rhizosphere are currently being processed for 16S rRNA amplicon sequencing in order to study the HAM recruitment and inheritance in these SBL deficient genotypes.

Figure 4 shows the *Hpa* infection quantified by number of *Hpa* (-10^5) spores in the conditioning population. Col-0 RPP5, which is completely resistant to *Hpa* isolate Noco2, showed no sporulation, as expected. This is significantly lower compared to Col-0 ($P < 0.05$, Tukey's post-hoc test). Coumarin and flavonoid deficient mutants *f6'h1* and *tt4* did not differ significantly from Col-0. However, camalexin deficient mutant *pad3* had a significantly higher ($P < 0.05$, Tukey's post-hoc test) spore count than Col-0, indicating an enhanced susceptibility to *Hpa* strain Noco2.

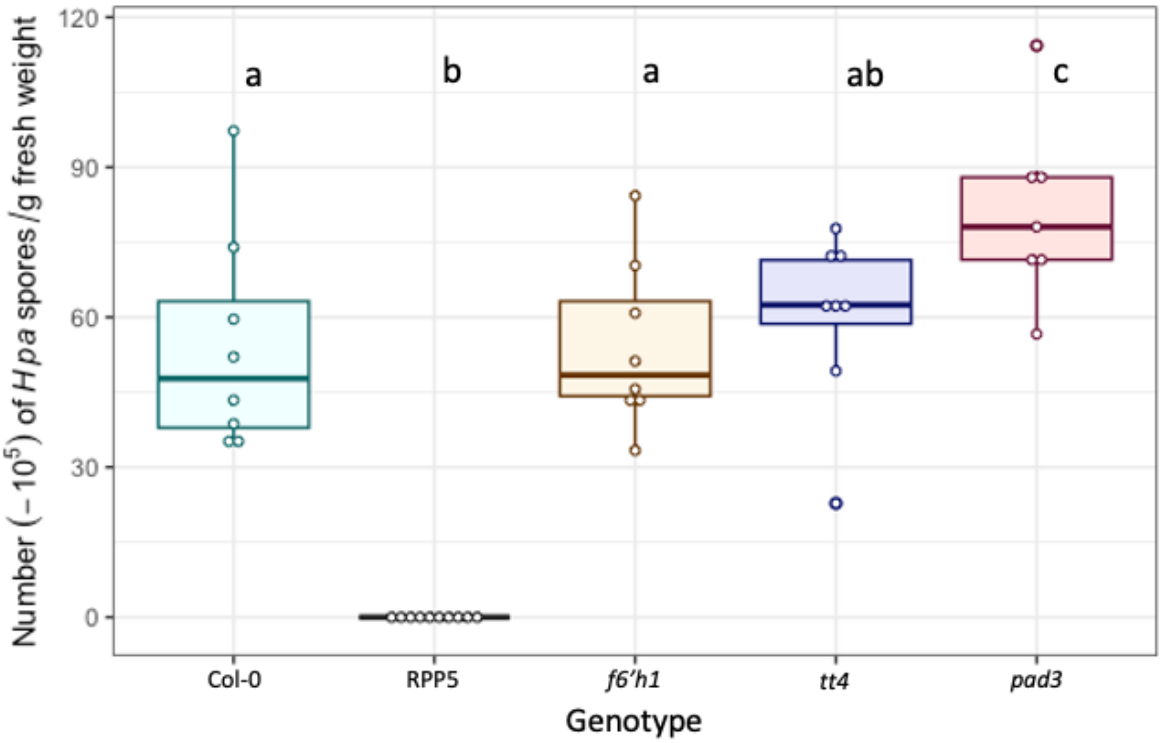

Figure 4. Disease severity in number (-10^5) of *Hpa* spores corrected for shoot fresh weight (g), of different *A. thaliana* genotypes grown on natural Reijerscamp soil, 7 days post *Hpa* inoculation. Significant differences are indicated with different letters ($P < 0.05$, Tukey's post-hoc test).

Bioluminescent XUU colonizes primary roots of several genotypes within 24h regardless of gno*Hpa* infection

Bioluminescent *Xanthomonas* strain (XUU), representative to the most prominent HAM ASV *Xanthomonas* a0e1a, was used to visualize the disease-induced recruitment of the HAM. In a plate setup, *A. thaliana* seedlings of genotypes Col-0, Col-0 RPP5, *f6'h1*, *tt4* and *pad3* were either mock-treated or inoculated with gno*Hpa*. XUU was inoculated on the root tip 3 days after gno*Hpa* inoculation, followed by daily imaging to follow the recruitment.

The distance of XUU colonization (mm) along the seedling root was measured at 1dpi (top row) and 2dpi (bottom row), of mock-treated (blue) and gno*Hpa*-inoculated (brown) seedlings (Fig. 5A). In all tested genotypes, gno*Hpa*-inoculated seedlings did not show increased XUU colonization compared to mock-treated seedlings ($P > 0.05$, one-tailed Welch's *t*-test), neither at 1dpi nor 2dpi. Based on these results, gno*Hpa* inoculation does not appear to increase XUU colonization regardless of genotype. However, the entire seedling root appeared to be colonized at 1dpi, the first timepoint of measurement. When tested for additional root colonization, using pairwise comparisons of seedlings between 1dpi and 2dpi, there were significant differences in XUU colonization distance ($P > 0.05$, Wilcoxon signed rank test), regardless of treatment and genotype (Fig. 5B). Indeed, this implies complete colonization of the root at 1dpi. Figure 5C shows CCD images of Col-0 seedlings on which the

colonization is clearly visible. At 1dpi, there is bioluminescence signal at the point of inoculation (white arrow) and the root-shoot junction (black arrow). This bioluminescence signal appears brighter at 2dpi as XUU continues to multiply adjacent to the seedling root (Fig. 5C). These results imply that XUU colonization happens within 1dpi, and potential differential colonization rates due to infection may occur at earlier timepoints.

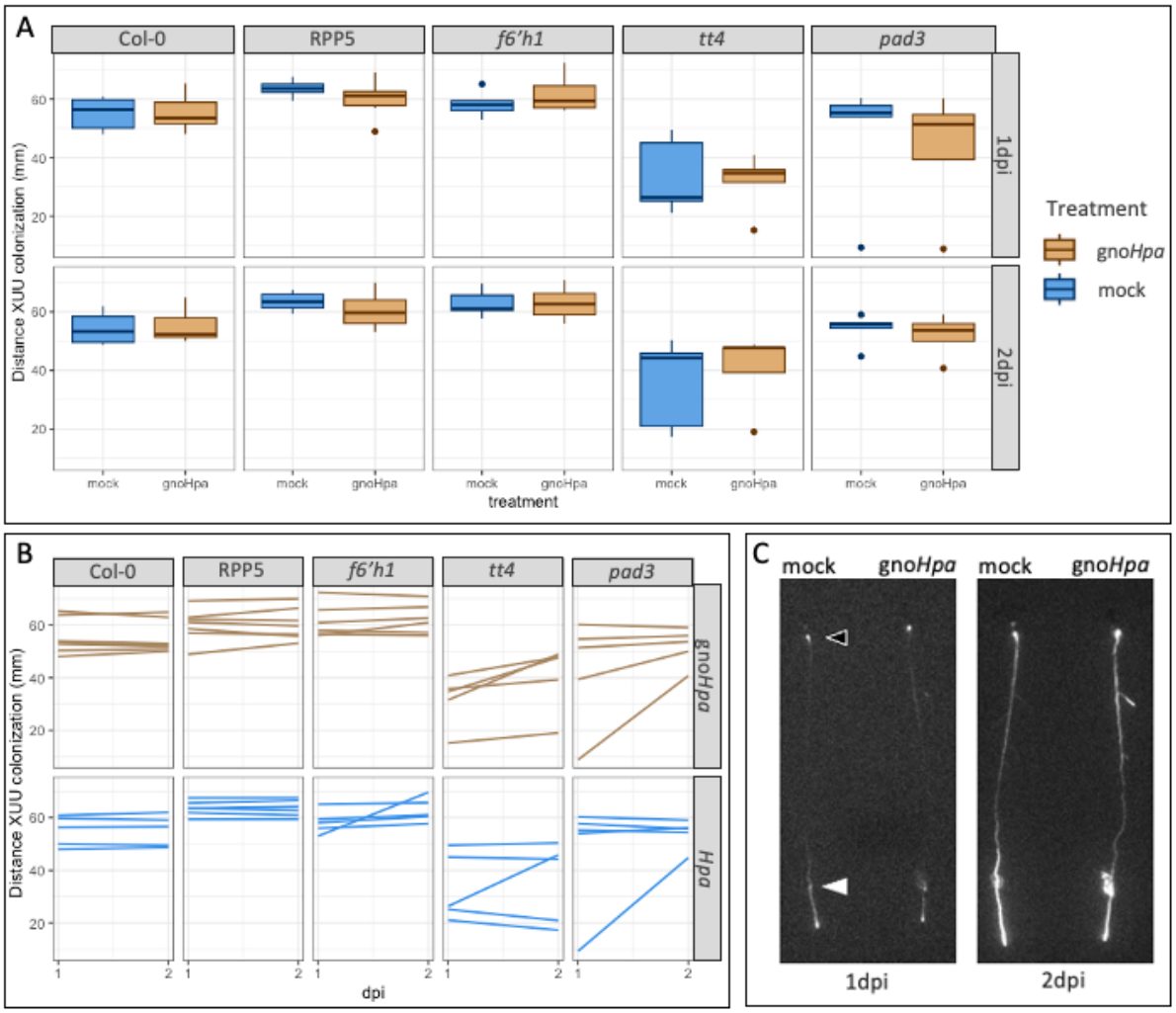

Figure 5. A) Distance of XUU colonization in mm along mock (blue) or gno*Hpa* (brown) treated Col-0, Col-0 RPP5, *f6'h1*, *tt4* or *pad3* seedling roots at 1 and 2 days post XUU inoculation. Within genotypes, XUU colonization distance was not significantly increased in gno*Hpa*-treated seedlings compared to mock treated seedlings ($P > 0.05$, one-tailed Welch's *t*-test). B) Distance of XUU colonization in mm from 1dpi to 2dpi along mock (blue) or gno*Hpa* (brown) treated Col-0, Col-0 RPP5, *f6'h1*, *tt4* or *pad3* seedling roots. Pairwise comparisons within genotype and treatment did not reveal significant differences between 1dpi and 2dpi ($P > 0.05$, Wilcoxon signed rank test). C) CCD images of bioluminescent XUU signal on mock and gno*Hpa*-treated Col-0 seedlings 1 and 2 dpi. Arrows indicate the XUU inoculation point (white) and the root-shoot junction (black).

Discussion

In this study, we aimed to gain more insight into the *Hpa*-induced recruitment and inheritance of beneficial microbes. To this end, we validated the microbial origin of SBL, demonstrated HAM buildup in *Hpa* laboratory cultures, elucidated the impact of root exudates on HAM inheritance, and visualized *Hpa*-induced recruitment with bioluminescent *Xanthomonas (XUU)*. First of all, we showed that SBL does not occur in sterilized soil, and amendment with natural soil microbes remediates SBL. Additionally, repeated passaging was shown to cause similar increasing patterns of (gno)*Hpa* infection in both gno*Hpa*- and *Hpa*-started mimic laboratory cultures, with no differences between gno*Hpa* and *Hpa* lines. Adjusting for previous infection rates resulted in ambiguous patterns of (gno)*Hpa* infection success rates in individual replicates. In a root exudate mutant SBL assay, camalexin deficient mutant *pad3* was shown to be highly susceptible to *Hpa* infection in the conditioning phase. In visualization assays with bioluminescent *XUU*, no differential colonization was found after 1 dpi, regardless of genotype or gno*Hpa* infection. Although there are no results yet on the microbial community compositions, as sequencing data is still being processed, this study increases the understanding of the roles that both microbes and plants play during (gno)*Hpa* infection.

Similar to approaches previously conducted by Cook & Rovira (1976) and Westphal & Becker (2000), we tested the possible theory that SBL may be directly influenced by plant-produced chemicals, rather than being the consequence of disease-induced recruitment of beneficial microbes (Berendsen *et al*., 2018) by eliminating soil microbes from natural Reijerscamp soil through Gamma-irradiation. Our results solidify the previous findings that SBL is indeed mediated by soil microbes, rather than a direct effect of plant root exudates, as SBL did not occur in sterilized soil, but could be remediated in a 1:9 mix of natural to sterilized soil (Fig. 1). The remediation of SBL with a low density microbial community further indicates that the microbes present in the natural soil are essential in this disease suppression. Despite this validation, it remains unclear where these microbes perform their beneficial effect, as HAM were found in both the rhizo- and the phyllosphere (Goossens & Spooren *et al*., 2023). Whether these microbes act by inducing systemic resistance through root colonization, or by colonizing the phyllosphere and locally impeding (gno)*Hpa* infection requires further research. Most likely, both modes of action apply, and future experiments should aim to clearly differentiate the two. For example, apart from testing for ISR marker genes (Pieterse *et al*., 2014), one could perform grafting experiments to study systemic signaling and reveal whether root-associated HAM induce systemic resistance (Tsutsui & Notaguchi, 2017). Additionally, *A. thaliana* plants could be inoculated with MAMPs of HAM members rather than a live community, as this is not expected to impact (gno)*Hpa* locally but may induce systemic resistance when the inoculum seeps into the soil. Discovering the exact mode of action of these beneficial microbes is a key step in understanding and harnessing their plant-aiding qualities.

Secondly, an experiment with mimic laboratory *Hpa* cultures, started with gno*Hpa* and *Hpa* and passaged every week for 5 weeks, showed increased *Hpa* infection in both lines in the last week compared to the first (Fig. 2). The increase can be explained by the natural multiplication of (gno)*Hpa* during infection, as a singular spore produces a sporangium with numerous spores (Slusarenko & Schlaich, 2003). After the initial inoculation, we did not count the number of spores in each inoculation, as this is time-costly and would create too much of a time bias throughout the inoculation day. Instead, qPCR was used as an accurate measure of the *Hpa* infection (Anderson & McDowell, 2015). Individual replicate lines generally showed an increase in *Hpa*/At ratio (Fig. S3), which can be attributed to the natural replication of *Hpa*. In a similar experiment, Ehau-Taumaunu & Hockett (2023) initially found an increase of bacterial speck disease when passaging the phyllosphere community in tomato. After 5 weeks, they found a strong suppression of bacterial speck disease, which was attributed to the development of a disease-suppressive phyllosphere microbial community (Ehau-Taumaunu & Hockett, 2023). However, when we adjusted for the *Hpa*/At DNA ratio of the previous week, the weekly *Hpa* infection success rate was not a unidirectional increase (Fig. 3). Both gno*Hpa* and *Hpa* lines showed

success rate variability, with most replicates increasing and decreasing throughout the experiment. Of particular interest are the replicates that have an *Hpa* infection success rate of 1 or lower, indicating a lack of progression in *Hpa* reproduction. The anticipated 16S rRNA sequencing data of those samples may reveal interesting phyllosphere microbes, possibly *Hpa*-associated, that play a role in disease suppression.

Thirdly, different SBL-deficient *Arabidopsis* mutants impaired in the production of coumarins, flavonoids and camalexins, were used to track the soil-borne inheritance of HAM that is thought to underly SBL (Goossens & Spooren *et al*., 2023). Compared to Col-0, camalexin-deficient mutant *pad3* was found to be highly susceptible to *Hpa* infection, more so than the other genotypes tested. Camalexin is a phytoalexin that originates in the roots but can act locally upon leaf pathogen infection (Koprivova *et al*., 2023). Its antimicrobial activity is pathogen specific, as *pad3* mutants were found to have enhanced susceptibility to eukaryote pathogens, such as *Alternaria brassiciola* and *Leptosphaeria maculans* (Thomma *et al*., 1999; Bohman *et al*., 2004), *Hpa* strain Hind4 (Glazebrook *et al., 1997)*, but not for *Pseudomonas syringae* (Zhou *et al*., 1999). This increased susceptibility had not yet been shown for Noco2, the *Hpa* strain used in this experiment. An impaired local response by *pad3* mutants may explain the increased *Hpa* spore count seen in this study. However, camalexin deficiency may also alter the microbial composition of the phyllosphere thereby indirectly affecting *Hpa* infection. The sequencing data will reveal how the phyllosphere microbial composition and abundance differs in *pad3* and the other root exudate mutants compared to Col-0. Additionally, the microbial composition of the rhizo- and phyllosphere of the response phase of this experiment will give insight into the inheritance of the beneficial microbes recruited in this conditioning phase.

Lastly, we used bioluminescence to visualize bacterial recruitment in planta, using a bioluminescence construct as described by Paauw *et al* (2023). A bioluminescent *Xanthomonas* strain (*XUU*) representative to the most prominent HAM ASV *Xanthomonas* a0e1a was used to visualize recruitment along the roots of different SBL-deficient genotypes. All genotypes had fully colonized roots within 1 day after inoculation (dpi) with XUU, in both gno*Hpa* and mock treated seedlings. Therefore, no differential colonization was found at 1dpi. If gno*Hpa* and mock treated seedlings are colonized at different speeds, this happens within the first 24h after inoculation. Therefore, future experiments should include visualizing *XUU* colonization multiple times within 24h of inoculation in order to study this possible differential colonization between gno*Hpa* and mock treated seedlings. Additionally, more variables should be considered in order to explain possible variability in *XUU* colonization. For example, disease quantification with a visual scoring system or even qPCR at the end of the experiment, may reveal varying colonization speeds. Instead of focusing solely on colonization speed, quantification of *XUU* may reveal a difference in multiplication rates depending on treatment or genotype of the seedlings, which needs to be considered as bacterial density is an important factor of population dynamics and effect on the plant (Raaijmakers *et al*., 2008). Furthermore, the use of bioluminescent *XUU* can be extended to inoculation on the phyllosphere, as described by Paauw *et al* (2023). By inoculating bioluminescent *XUU* onto the leaves along with (gno)*Hpa*, its localization and perceived effect on infection can be studied in detail. With these proposed improvements, we can further elucidate the localization and action of HAM ASVs using this *Xanthomonas* representative.

The current hypothesis for SBL is that upon foliar infection with gno(*Hpa*), plants recruit beneficial soil microbes to their rhizosphere, and that a subsequent plant population inherits these microbes to their roots and leaves where they induce resistance. Although the HAM ASV that *XUU* represents was previously associated with the phyllosphere (Goossens & Spooren *et al*., 2023), no bioluminescent *XUU* signal was found on shoot or leaf material in this plate experiment, as colonization appeared to stop at the root shoot junction. *XUU* may have colonized the shoot and leaf material, possibly via the endosphere, but the bioluminescent signal was not detectable. This can be explained by suboptimal growth conditions of the phyllosphere compared to the root and growth medium, which likely

supported the strong growth of bioluminescent *XUU* along the seedling root. However, another possible explanation for the previously found phyllosphere HAM in response populations (Goossens & Spooren *et al*., 2023) is not the transfer of bacteria from root to shoot, but rather the germination of seeds directly on conditioned soil. In common bean, soybean, and canola cultivars, early season phyllosphere microbiomes were found to consist largely of soil-associated microbes, whereas later timepoints revealed a more limited microbiome of mainly phyllosphere resident bacteria (Copeland *et al*., 2014). This indicates an inheritance of soil-microbes in the phyllosphere through direct contact during germination, which fades overtime as the leaves are exposed to varying temperature, humidity, and UV-radiation (Koskella, 2020). In an SBL setting, this hypothesis can be tested by laying a permeable barrier (e.g. tissue paper) over conditioned soil, on which seeds are sown. That way, the shoot and leaf material remains free of soil microbes, while the root can grow through the barrier and into the soil. One may do this experiment using a synthetic community (representative) of HAM members and performing qPCRs to determine which HAM members dominate. Subsequently, one may use drop-out experiments to discover which specific microbes are effective at causing ISR and/or SBL, as described by Finkel *et al* (2020). Finding these specific beneficial microbes that aid the plant against *Hpa* infection and elucidating how they arrive on the phyllosphere are the next step in understanding these intricate interactions.

In conclusion, this study shows that SBL is dependent on microbes, although much about their recruitment and inheritance remains unclear. The anticipated 16S rRNA sequencing data is expected to reveal how gno*Hpa* and *Hpa* mimic laboratory cultures phyllosphere microbiomes developed over time, and whether *pad3* enhanced susceptibility is correlated with a change in microbial composition. These results, along with future experiments on the exact mechanisms of HAM recruitment and inheritance, are important to increase our understanding of the relationship between plants, beneficial microbes, and pathogenic oomycetes. Ultimately, this will help enable the development of sustainable biological control methods against pathogenic oomycetes in food crops.

References

1. Anderson, R. G., & McDowell, J. M. (2015). A PCR assay for the quantification of growth of the oomycete pathogen *Hyaloperonospora arabidopsidis* in *Arabidopsis thaliana*: A qPCR assay for *Hyaloperonospora arabidopsidis*. *Molecular Plant Pathology*, *16*(8), 893–898. https://doi.org/10.1111/mpp.12247
2. Andrews, J. H. (1992). Biological control in the phyllosphere. *Annual Review of Phytopathology*, *30*, 603–635. https://doi.org/10.1146/annurev.py.30.090192.003131
3. Bakker, P. A. H. M., Pieterse, C. M. J., de Jonge, R., & Berendsen, R. L. (2018). The Soil-Borne Legacy. *Cell*, *172*(6), 1178–1180. https://doi.org/10.1016/j.cell.2018.02.024
4. Berendsen, R. L., Pieterse, C. M. J., & Bakker, P. A. H. M. (2012). The rhizosphere microbiome and plant health. *Trends in Plant Science*, *17*(8), 478–486. https://doi.org/10.1016/j.tplants.2012.04.001
5. Berendsen, R. L., Vismans, G., Yu, K., Song, Y., de Jonge, R., Burgman, W. P., Burmølle, M., Herschend, J., Bakker, P. A. H. M., & Pieterse, C. M. J. (2018). Disease-induced assemblage of a plant-beneficial bacterial consortium. *The ISME Journal*, *12*(6), Article 6. https://doi.org/10.1038/s41396-018-0093-1
6. Bohman, S., Staal, J., Thomma, B. P. H. J., Wang, M., & Dixelius, C. (2004). Characterisation of an Arabidopsis–Leptosphaeria maculans pathosystem: Resistance partially requires camalexin biosynthesis and is independent of salicylic acid, ethylene and jasmonic acid signalling. The Plant Journal, 37(1), 9–20. https://doi.org/10.1046/j.1365-313X.2003.01927.x
7. Boller, T., & Felix, G. (2009). A Renaissance of Elicitors: Perception of Microbe-Associated Molecular Patterns and Danger Signals by Pattern-Recognition Receptors. *Annual Review of Plant Biology*, *60*(1), 379–406. https://doi.org/10.1146/annurev.arplant.57.032905.105346

8. Coates, M. E., & Beynon, J. L. (2010). *Hyaloperonospora arabidopsidis* as a Pathogen Model. *Annual Review of Phytopathology*, *48*(1), 329–345. https://doi.org/10.1146/annurev-phyto-080508-094422
9. Cook, R. J., & Rovira, A. D. (1976). The role of bacteria in the biological control of Gaeumannomyces graminis by suppressive soils. *Soil Biology and Biochemistry*, *8*(4), 269–273. https://doi.org/10.1016/0038-0717(76)90056-0
10. Copeland, J. K., Yuan, L., Layeghifard, M., Wang, P. W., & Guttman, D. S. (2015). Seasonal Community Succession of the Phyllosphere Microbiome. *Molecular Plant-Microbe Interactions®*, *28*(3), 274–285. https://doi.org/10.1094/MPMI-10-14-0331-FI
11. Ehau-Taumaunu, H., & Hockett, K. L. (2022). Passaging Phyllosphere Microbial Communities Develop Suppression Towards Bacterial Speck Disease in Tomato. *Phytobiomes Journal*, PBIOMES-05-22-0030-FI. https://doi.org/10.1094/PBIOMES-05-22-0030-FI
12. Glazebrook, J., Zook, M., Mert, F., Kagan, I., Rogers, E. E., Crute, I. R., Holub, E. B., Hammerschmidt, R., & Ausubel, F. M. (1997). Phytoalexin-Deficient Mutants of Arabidopsis Reveal That *PAD4* Encodes a Regulatory Factor and That Four *PAD* Genes Contribute to Downy Mildew Resistance. *Genetics*, *146*(1), 381–392. https://doi.org/10.1093/genetics/146.1.381
13. Goossens, P., Spooren, J., Baremans, K. C. M., Andel, A., Lapin, D., Echobardo, N., Pieterse, C. M. J., Van Den Ackerveken, G., & Berendsen, R. L. (2023). *Congruent downy mildew-associated microbiomes reduce plant disease and function as transferable resistobiomes* [Preprint]. Microbiology. https://doi.org/10.1101/2023.03.14.532520
14. Hardoim, P. R., van Overbeek, L. S., & Elsas, J. D. van. (2008). Properties of bacterial endophytes and their proposed role in plant growth. *Trends in Microbiology*, *16*(10), 463–471. https://doi.org/10.1016/j.tim.2008.07.008
15. Hassan, S., & Mathesius, U. (2012). The role of flavonoids in root–rhizosphere signalling: Opportunities and challenges for improving plant–microbe interactions. *Journal of Experimental Botany*, *63*(9), 3429–3444. https://doi.org/10.1093/jxb/err430
16. Koprivova, A., Schuck, S., Jacoby, R. P., Klinkhammer, I., Welter, B., Leson, L., Martyn, A., Nauen, J., Grabenhorst, N., Mandelkow, J. F., Zuccaro, A., Zeier, J., & Kopriva, S. (2019). Root-specific camalexin biosynthesis controls the plant growth-promoting effects of multiple bacterial strains. *Proceedings of the National Academy of Sciences of the United States of America*, *116*(31), 15735–15744. https://doi.org/10.1073/pnas.1818604116
17. Koskella, B. (2020). The phyllosphere. *Current Biology*, *30*(19), R1143–R1146. https://doi.org/10.1016/j.cub.2020.07.037
18. Meena, M., Swapnil, P., Zehra, A., Aamir, M., Dubey, M. K., Goutam, J., & Upadhyay, R. S. (2017). Beneficial Microbes for Disease Suppression and Plant Growth Promotion. In D. P. Singh, H. B. Singh, & R. Prabha (Eds.), *Plant-Microbe Interactions in Agro-Ecological Perspectives: Volume 2: Microbial Interactions and Agro-Ecological Impacts* (pp. 395–432). Springer. https://doi.org/10.1007/978-981-10-6593-4_16
19. Murashige, T., & Skoog, F. (1962). A Revised Medium for Rapid Growth and Bio Assays with Tobacco Tissue Cultures. *Physiologia Plantarum*, *15*(3), 473–497. https://doi.org/10.1111/j.1399-3054.1962.tb08052.x
20. Pascale, A., Proietti, S., Pantelides, I. S., & Stringlis, I. A. (2020). Modulation of the Root Microbiome by Plant Molecules: The Basis for Targeted Disease Suppression and Plant Growth Promotion. *Frontiers in Plant Science*, *10*. https://www.frontiersin.org/articles/10.3389/fpls.2019.01741
21. Paauw, M., van Hulten, M., Chatterjee, S., Berg, J. A., Taks, N. W., Giesbers, M., Richard, M. M. S., & van den Burg, H. A. (2023). Hydathode immunity protects the Arabidopsis leaf vasculature against colonization by bacterial pathogens. *Current Biology*, *33*(4), 697-710.e6. https://doi.org/10.1016/j.cub.2023.01.013
22. Pieterse, C. M., van Wees, S. C., Hoffland, E., van Pelt, J. A., & van Loon, L. C. (1996). Systemic resistance in Arabidopsis induced by biocontrol bacteria is independent of salicylic acid

accumulation and pathogenesis-related gene expression. *The Plant Cell*, *8*(8), 1225–1237. https://doi.org/10.1105/tpc.8.8.1225
23. Pieterse, C. M. J., Zamioudis, C., Berendsen, R. L., Weller, D. M., Van Wees, S. C. M., & Bakker, P. A. H. M. (2014). Induced systemic resistance by beneficial microbes. *Annual Review of Phytopathology*, *52*, 347–375. https://doi.org/10.1146/annurev-phyto-082712-102340
24. Raaijmakers, J. M., & Mazzola, M. (2016). Soil immune responses. *Science*, *352*(6292), 1392–1393. https://doi.org/10.1126/science.aaf3252
25. Raaijmakers, J. M., Paulitz, T. C., Steinberg, C., Alabouvette, C., & Moënne-Loccoz, Y. (2009). The rhizosphere: A playground and battlefield for soilborne pathogens and beneficial microorganisms. *Plant and Soil*, *321*(1), 341–361. https://doi.org/10.1007/s11104-008-9568-6
26. Rolfe, S. A., Griffiths, J., & Ton, J. (2019). Crying out for help with root exudates: Adaptive mechanisms by which stressed plants assemble health-promoting soil microbiomes. *Current Opinion in Microbiology*, *49*, 73–82. https://doi.org/10.1016/j.mib.2019.10.003
27. Slusarenko, A. J., & Schlaich, N. L. (2003). Downy mildew of Arabidopsis thaliana caused by Hyaloperonospora parasitica (formerly Peronospora parasitica). *Molecular Plant Pathology*, *4*(3), 159–170. https://doi.org/10.1046/j.1364-3703.2003.00166.x
28. Stringlis, I. A., de Jonge, R., & Pieterse, C. M. J. (2019). The Age of Coumarins in Plant–Microbe Interactions. *Plant and Cell Physiology*, *60*(7), 1405–1419. https://doi.org/10.1093/pcp/pcz076
29. Thomma, B. P. H. J., Nelissen, I., Eggermont, K., & Broekaert, W. F. (1999). Deficiency in phytoalexin production causes enhanced susceptibility of Arabidopsis thaliana to the fungus Alternaria brassicicola. *The Plant Journal*, *19*(2), 163–171. https://doi.org/10.1046/j.1365-313X.1999.00513.x
30. Trivedi, P., Leach, J. E., Tringe, S. G., Sa, T., & Singh, B. K. (2020). Plant–microbiome interactions: From community assembly to plant health. *Nature Reviews Microbiology*, *18*(11), Article 11. https://doi.org/10.1038/s41579-020-0412-1
31. Tsutsui, H., & Notaguchi, M. (2017). The Use of Grafting to Study Systemic Signaling in Plants. *Plant and Cell Physiology*, *58*(8), 1291–1301. https://doi.org/10.1093/pcp/pcx098
32. Turner, T. R., James, E. K., & Poole, P. S. (2013). The plant microbiome. *Genome Biology*, *14*(6), 209. https://doi.org/10.1186/gb-2013-14-6-209
33. Vismans, G., Spooren, J., Pieterse, C. M. J., Bakker, P. A. H. M., & Berendsen, R. L. (2021). Soil-Borne Legacies of Disease in Arabidopsis thaliana. In L. C. Carvalhais & P. G. Dennis (Eds.), *The Plant Microbiome: Methods and Protocols* (pp. 209–218). Springer US. https://doi.org/10.1007/978-1-0716-1040-4_17
34. Vismans, G., van Bentum, S., Spooren, J., Song, Y., Goossens, P., Valls, J., Snoek, B. L., Thiombiano, B., Schilder, M., Dong, L., Bouwmeester, H. J., Pétriacq, P., Pieterse, C. M. J., Bakker, P. A. H. M., & Berendsen, R. L. (2022). Coumarin biosynthesis genes are required after foliar pathogen infection for the creation of a microbial soil-borne legacy that primes plants for SA-dependent defenses. *Scientific Reports*, *12*(1), Article 1. https://doi.org/10.1038/s41598-022-26551-x
35. Vorholt, J. A. (2012). Microbial life in the phyllosphere. *Nature Reviews Microbiology*, *10*(12), Article 12. https://doi.org/10.1038/nrmicro2910
36. Westphal, A., & Becker, J. O. (2000). Transfer of Biological Soil Suppressiveness Against Heterodera schachtii. *Phytopathology®*, *90*(4), 401–406. https://doi.org/10.1094/PHYTO.2000.90.4.401
37. Zhou, N., Tootle, T. L., & Glazebrook, J. (1999). Arabidopsis PAD3, a gene required for camalexin biosynthesis, encodes a putative cytochrome P450 monooxygenase. *The Plant Cell*, *11*(12), 2419–2428. https://doi.org/10.1105/tpc.11.12.2419

Supplemental figures

Shoot fresh weight and conditioning phase spore counts equal among inoculation and soil type

Shoot fresh weight did not differ significantly ($P > 0.05$, Tukey's post-hoc test) within soil types and between inoculation treatments in both the conditioning (Fig S1A) and the response population (Fig S1B). The disease severity of gno*Hpa* inoculated plants was statistically the same ($P > 0.05$, Tukey's post-hoc test) among all 3 soil types in the conditioning population (Fig S1C).

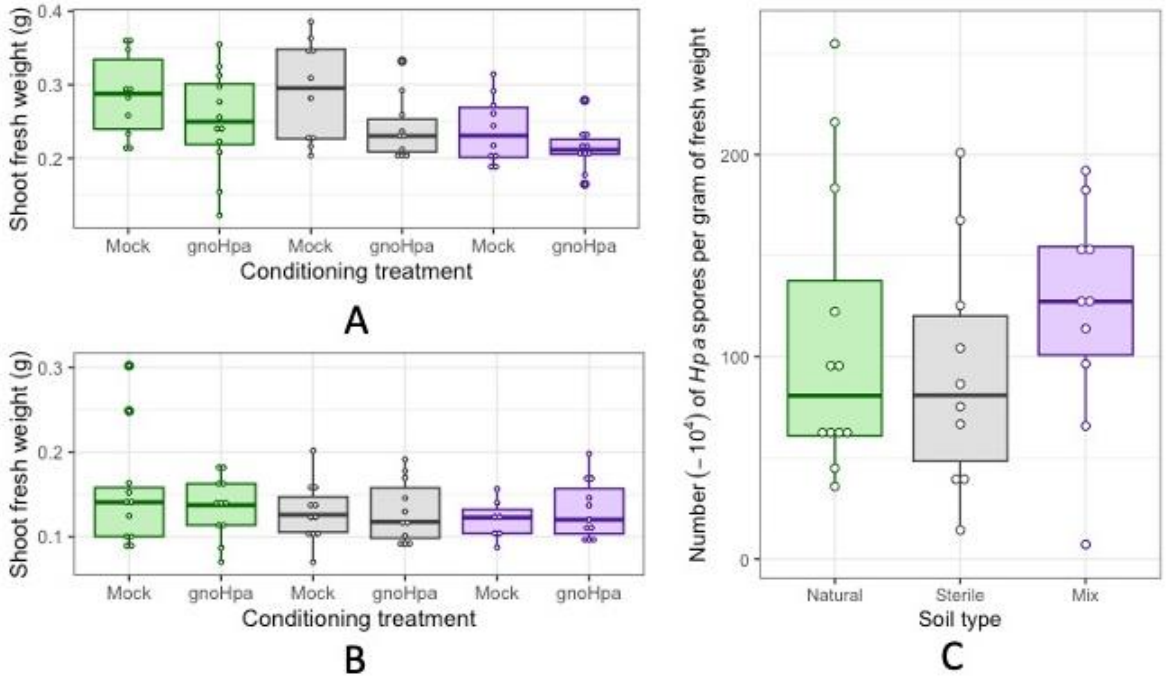

Fig S1. A) Shoot fresh weight (g) of the conditioning population, consisting of mock or gnoHpa inoculated plants, grown on natural (green), Gamma-irradiated (grey), or mix (purple) Reijerscamp soil. No statistical differences were found within soil types ($P > 0.05$, Tukey's post-hoc test). B) Shoot fresh weight (g) of the response population, consisting of gnoHpa inoculated plants, growing on mock or gnoHpa-conditioned natural (green), Gamma-irradiated (grey), or mix (purple) Reijerscamp soil. No statistical differences were found within soil types ($P > 0.05$, Tukey's post-hoc test). C) Disease severity of the gno*Hpa* inoculated conditioning population, corrected for fresh weight. No statistical differences were found between soil types ($P > 0.05$, Tukey's post-hoc test).

Increase in (gno)*Hpa* infection of one week correlates significantly with the infection rate of the previous week

A steady increase in (gno)*Hpa* infection was found over the course of the experiment, which can likely be attributed to the natural multiplication of (gno)*Hpa*. To test this hypothesis, we compared every week of the experiment with the previous week, to see whether there is indeed a positive correlation between the ratios of (gno)*Hpa*/At DNA. In every comparison, except in week 4 vs. week 3 in the (gno)*Hpa* line, and week 3 vs. week 2 in the *Hpa* line, there was a significant positive correlation (Fig. S2, $P < 0.05$, Pearson's correlation test). However, the comparison in week 4 vs. week 3 in the (gno)*Hpa* line does show a trend towards positive correlation ($P = 0.114$, Pearson's correlation test). Unexpectedly, there is clearly no correlation between week 3 and week 2 in the *Hpa* line. This could be attributed to a sudden shift in phyllosphere microbial composition, which the anticipated 16S rRNA sequencing data may reveal.

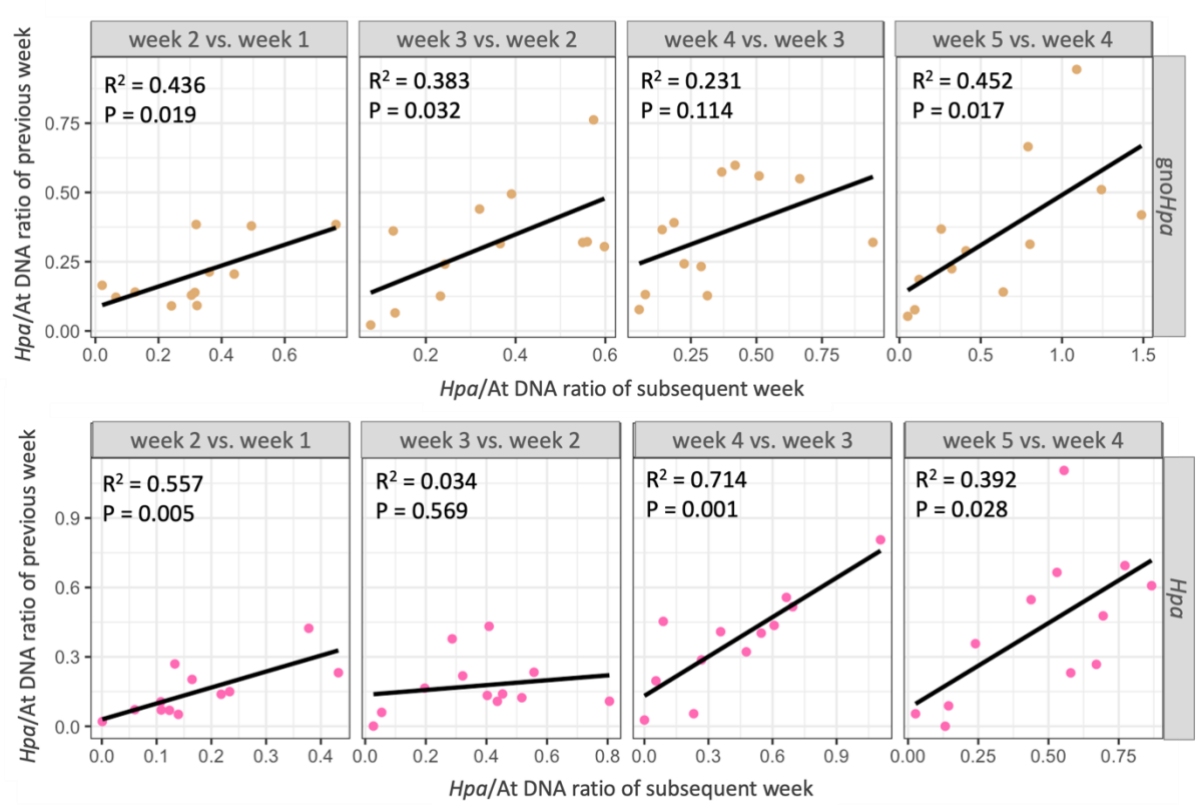

Fig S2. Scatter plots depicting the correlation between the *Hpa* of a subsequent week and a previous week, as depicted in the labels above each graph. Statistics were determined using Pearson's correlation test.

Unadjusted (gno)*Hpa* infection rate increases during passaging

When the (gno)*Hpa*/At ratio is not adjusted for (gno)*Hpa*/At ratio of the previous week, the individual replicates generally show a pattern of increase, with some replicates increasing more steeply than others (Fig. S3). This is likely due to the natural reproduction cycle of (gno)*Hpa*, which increases the quantity of spores with each passage.

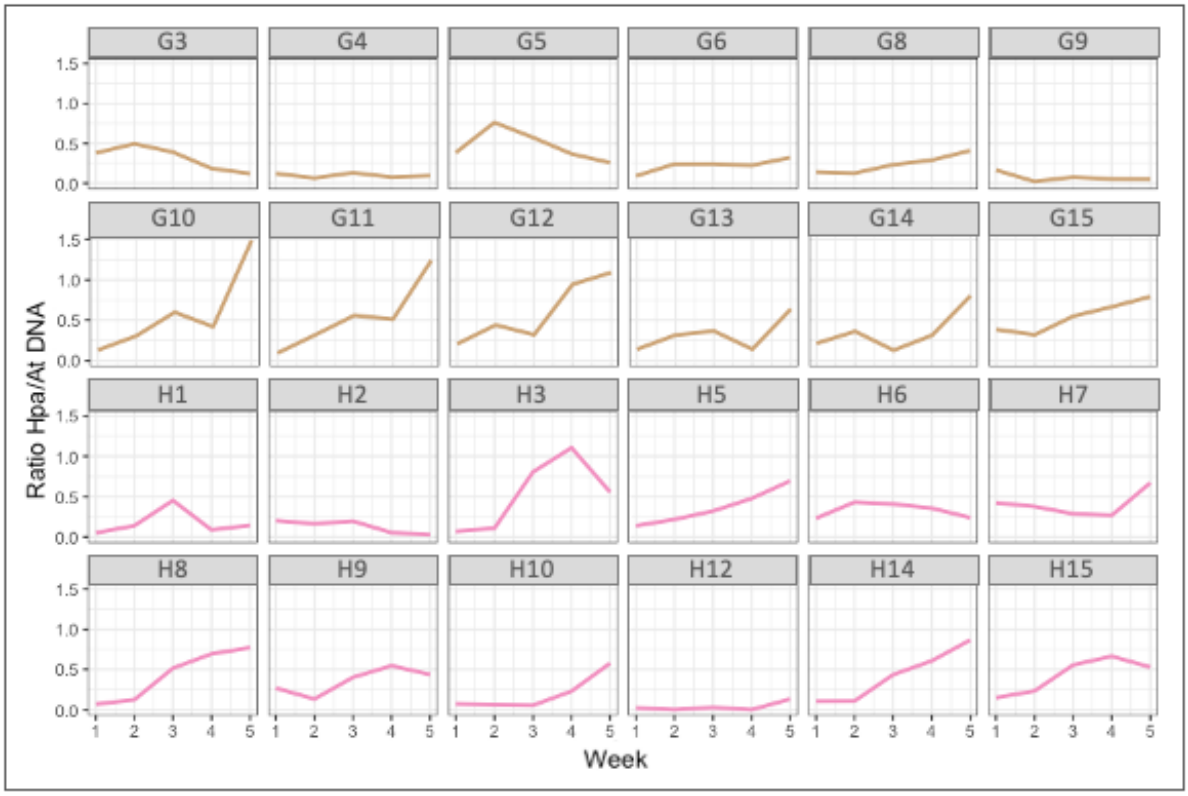

Fig S3. Weekly (gno)*Hpa*/At DNA ratio of individual replicates of gno*Hpa* (G, orange) and *Hpa* (H, pink) lines.